Electronic Supplementary Information (ESI) for

Construction of Di- and Tetra-ferrocenyl Spiroborate Complexes from Catechol Building Blocks and their Redox Behaviors

Keishiro Tahara,[a,*] Tetsuhiro Akita,[a] Shohei Katao[a] and Jun-ichi Kikuchi[a,*]

[a]*Graduate School of Materials Science, Nara Institute of Science and Technology, Ikoma 630-0192, Japan*

Contents

1. X-ray Crystallographic Data and Structure Data

Table S1. Summary of crystallographic data and refinement parameters for **3**.

empirical formula	$C_{28}H_{26}O_2Fe_2$
formula weight	506.21
crystal dimensions (mm)	0.130 x 0.120 x 0.110
crystal system	monoclinic
space group	$P2_1/n$ (#14)
temp (°C)	–150
a (Å)	15.1307(3)
b (Å)	7.4114(2)
c (Å)	20.2153(4)
β (deg)	100.8429(7)
V (Å^3)	2226.47(7)
Z	4
ρ_{calcd} (g cm^{-3})	1.510
F(000)	1048.00
μ (MoK$_\alpha$) (cm^{-1})	13.251
$2\phi_{max}$ (deg)	61.0
GOF	1.193
R1[a]	0.0305
wR2[b]	0.0804
$\Delta\rho_{max}/\Delta\rho_{min}$ (e/Å^3)	1.00/–0.42

[a] $R1 = \Sigma ||F_o| - |F_c|| / \Sigma |F_o|$. [b] $wR2 = [\Sigma (w(F_o^2 - F_c^2)^2) / \Sigma w(F_o^2)^2]^{1/2}$.

Table S2. Selected bond distances and angles for **3**.

	Å		Deg
C4-C5	1.4813(15)	C3-C4-C5	117.63(9)
C18-C19	1.4784(16)	C5-C4-C18	123.29(10)
C2-C3	1.3813(15)	C17-C18-C19	117.25(9)
C3-C4	1.4093(16)	C4-C18-C19	124.12(10)
C4-C18	1.4030(14)	C4-C5-C9	124.07(10)
C17-C18	1.4121(15)	C4-C5-C6	128.57(10)
C16-C17	1.3810(16)	C18-C19-C23	129.00(9)
C2-C16	1.4124(14)	C18-C19-C20	124.12(9)
C2-O1	1.3640(15)	C3-C4-C18	118.96(10)
C16-O2	1.3668(14)	C2-C3-C4	121.90(9)
C1-O1	1.4290(14)	C3-C2-C16	119.25(10)
C15-O2	1.4204(16)	C2-C16-C17	119.25(10)
		C16-C17-C18	121.98(9)
		C4-C18-C17	118.63(10)
		C17-C16-O2	125.47(9)
		C2-C16-O2	115.27(10)
		C16-C2-O1	115.43(9)
		C3-C2-O1	125.30(9)
		C15-O2-C16	116.90(10)
		C1-O1-C2	116.79(10)
		C5-C4-C18-C19	-2.76(15)

2. ^{1}H- and ^{13}C-NMR Spectra of New Compounds

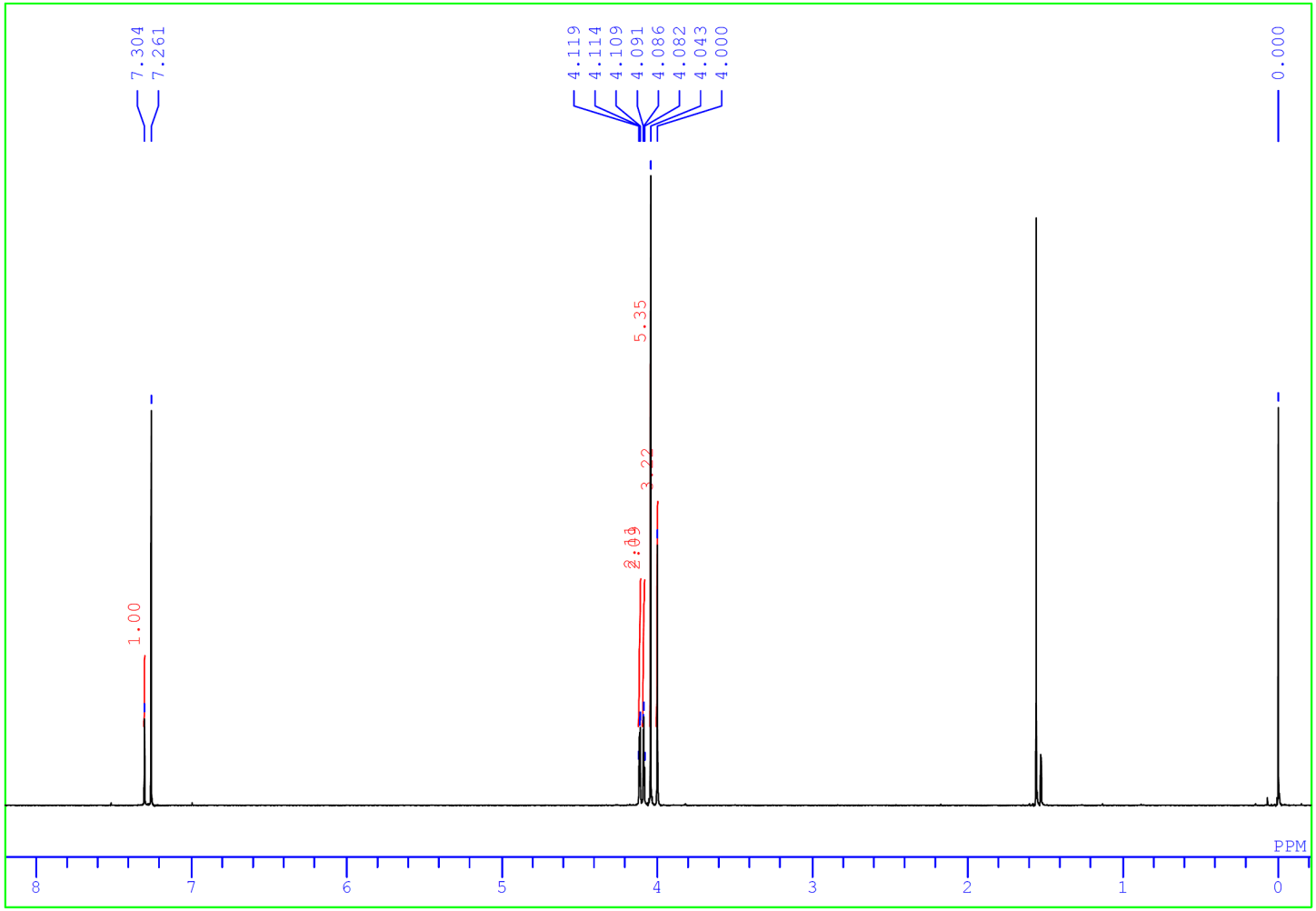

Fig. S1 ^{1}H-NMR spectrum of **3** in $CDCl_3$.

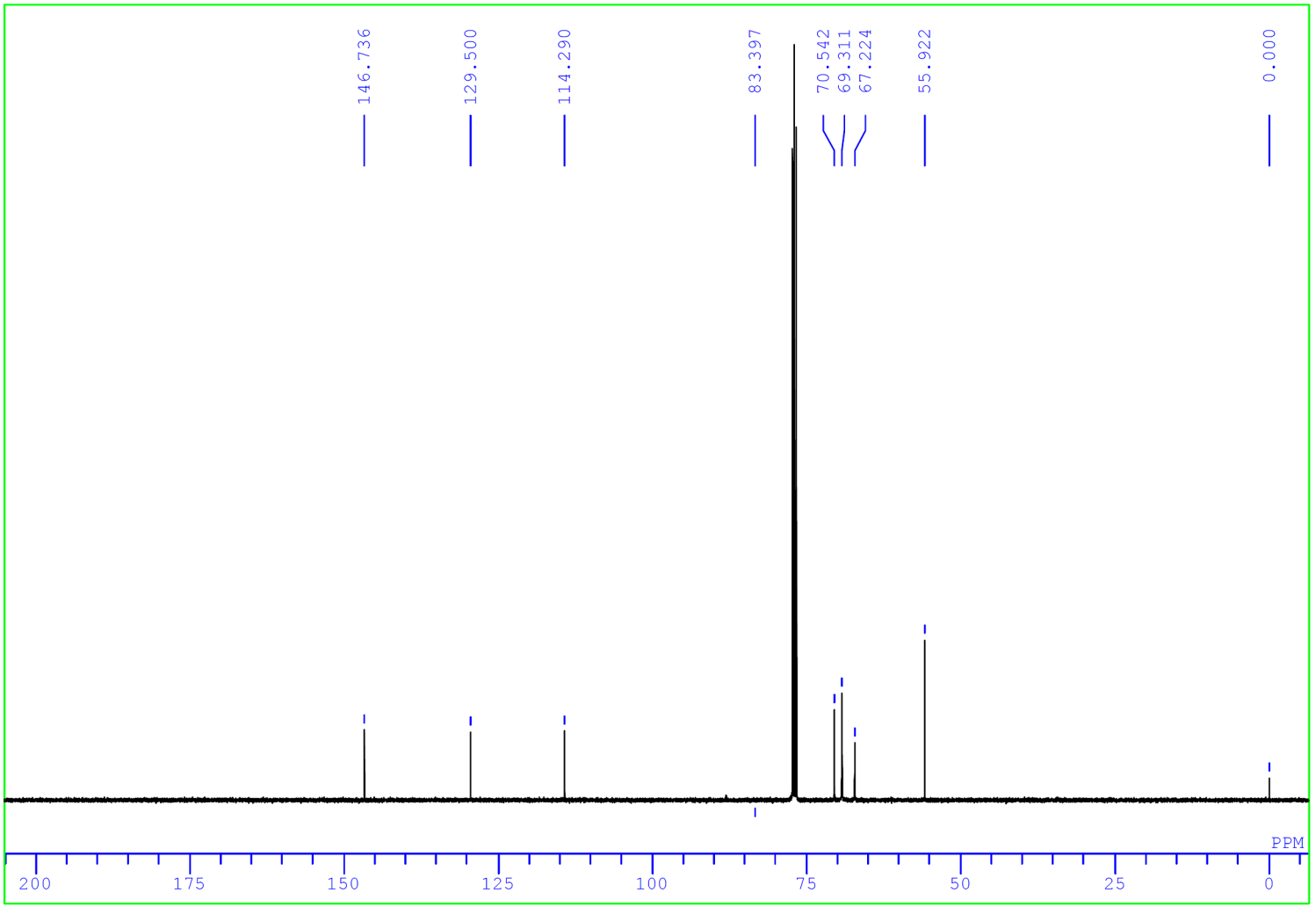

Fig. S2 ^{13}C-NMR spectrum of **3** in $CDCl_3$.

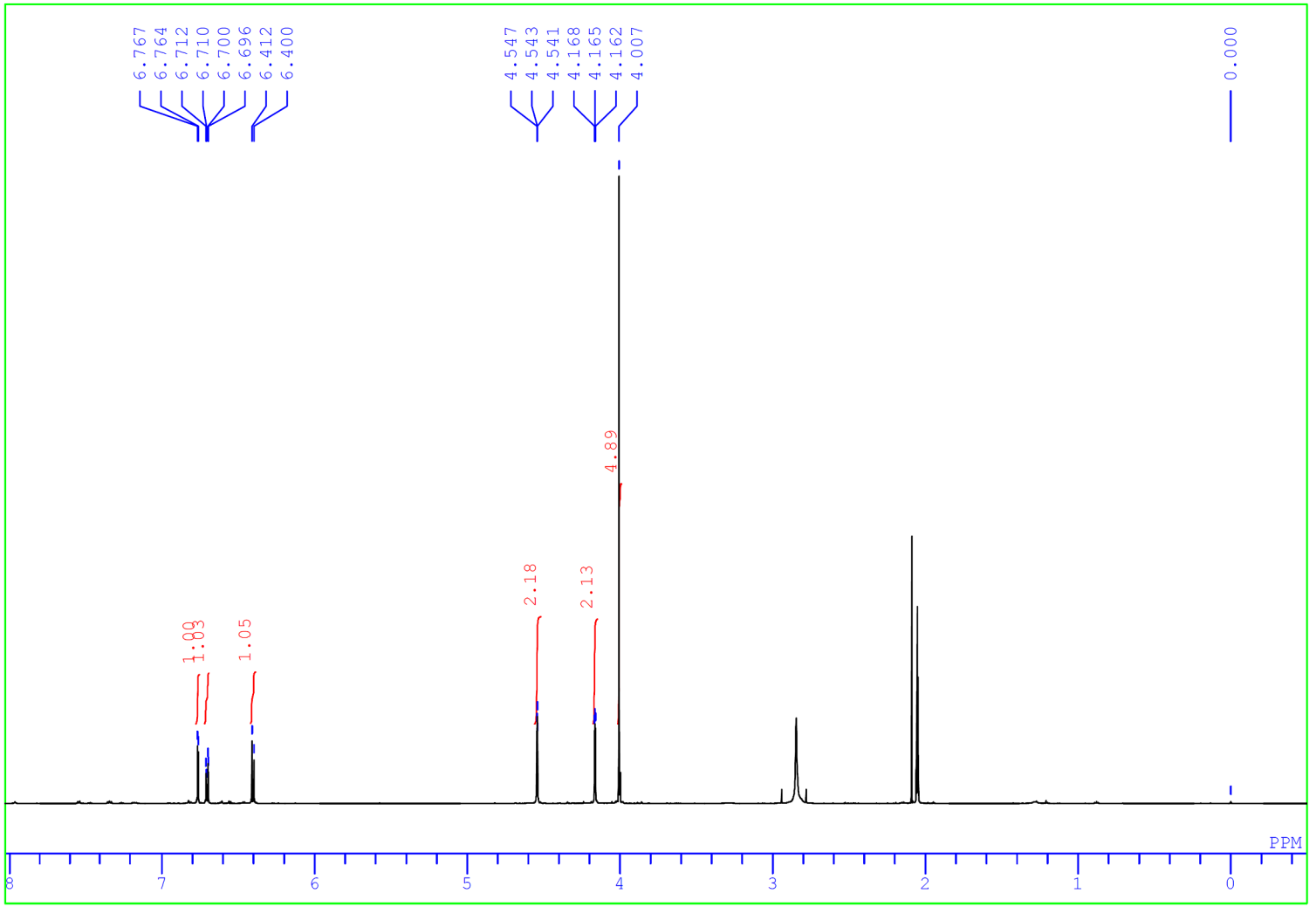

Fig. S3 ^{1}H-NMR spectrum of **K2** in acetone-d_6.

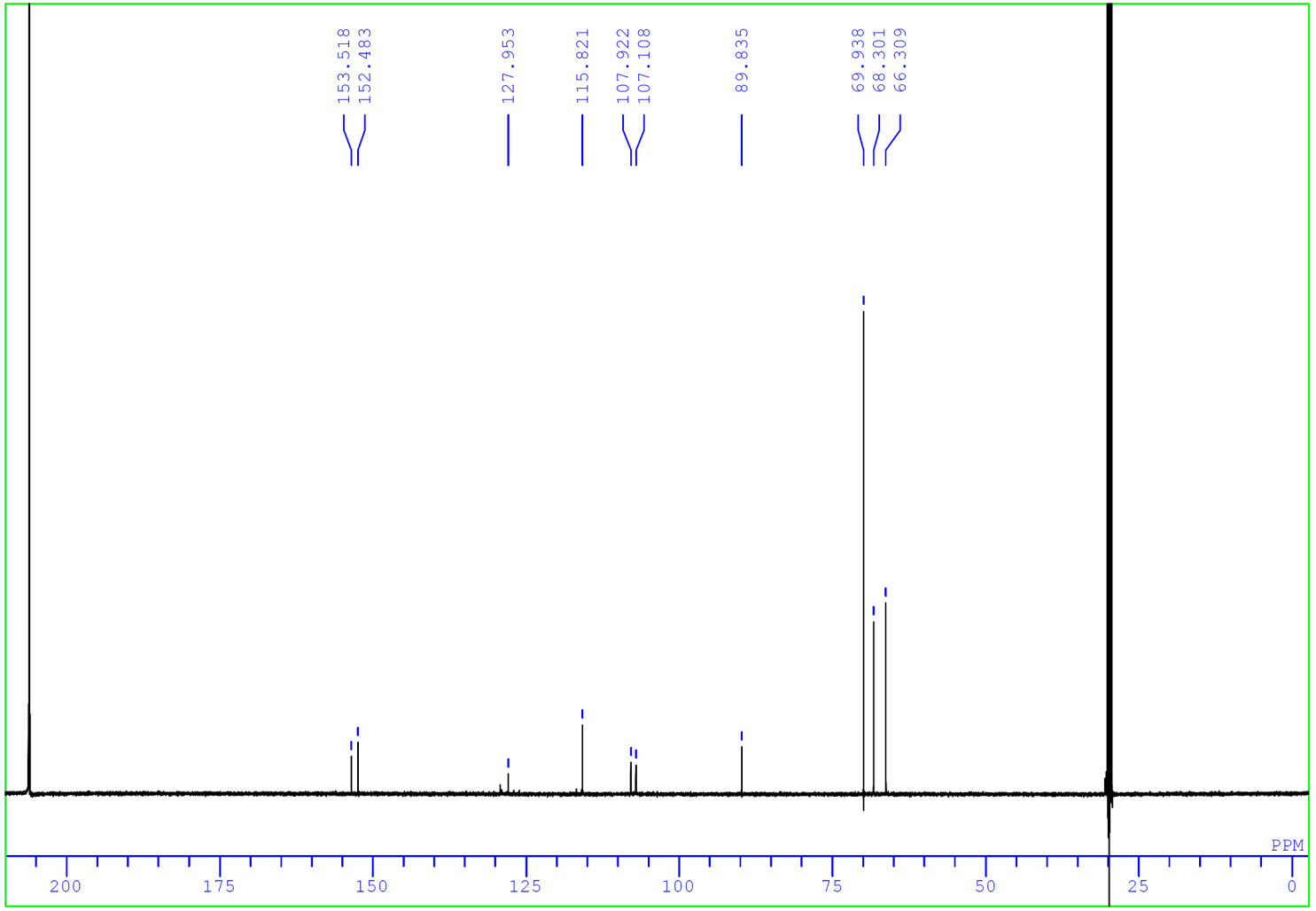

Fig. S4 ^{13}C-NMR spectrum of **K2** in acetone-d_6.

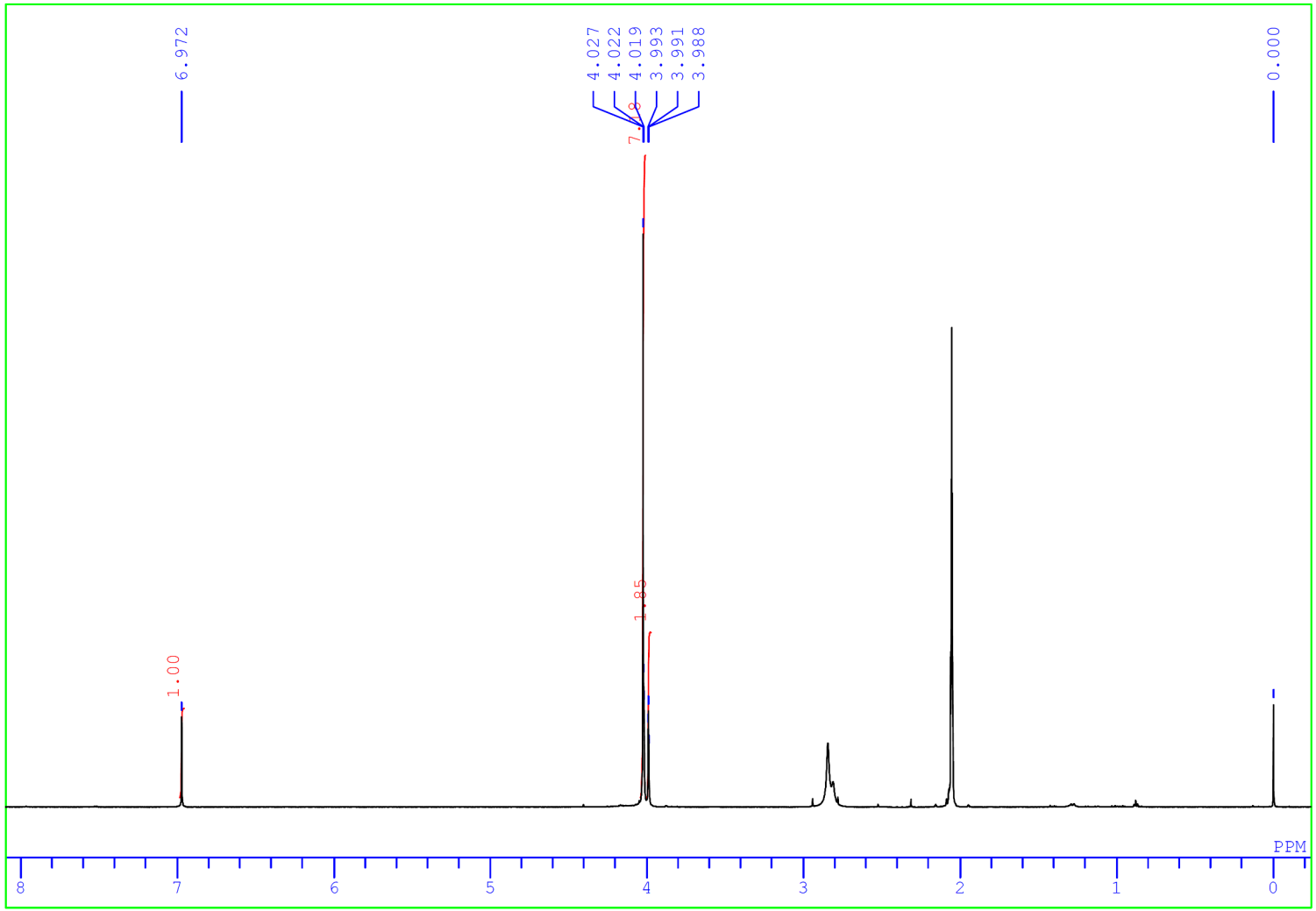

Fig. S5 ^{1}H-NMR spectrum of **K4** in acetone-d_6.

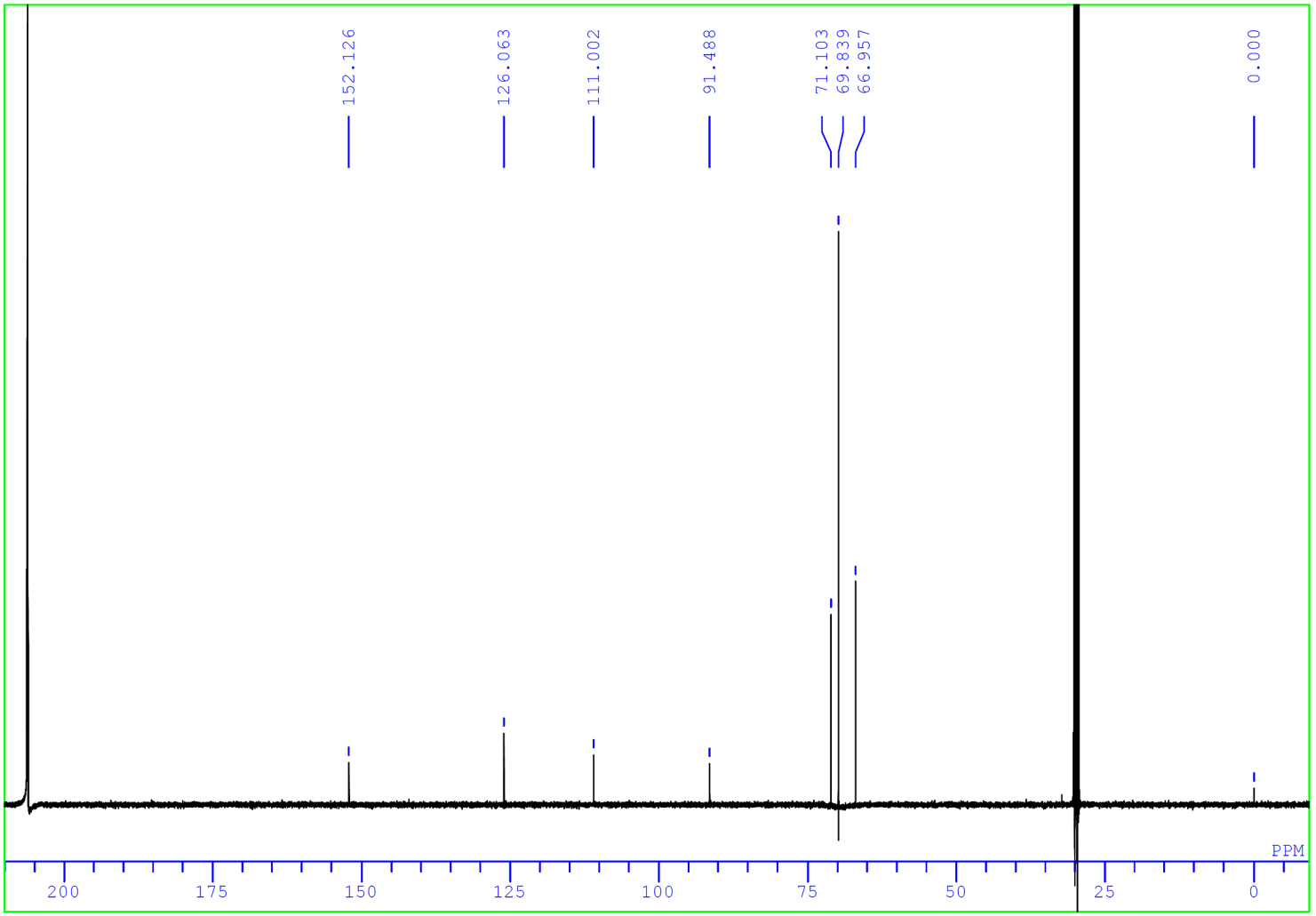

Fig. S6 ^{13}C-NMR spectrum of **K4** in acetone-d_6.

3. Differential NOE Experiment

To assign the ^{1}H signals of the C_5H_4 Cp ring (numbered as 2a and 2b in Scheme 1), we have performed 2D NMR measurements including HMQC and HMBC. Unfortunately, in the HMBC measurements, the C-H correlation between the ipso carbon of the benzene ring and 2a proton was not observed for the solutions of **1**, **3**, **K2** and **K4**. Thus, we performed 1D ^{1}H-NMR differential NOE experiments. Upon irradiation at the proton (numbered as 1 or 1a), enhancements of NOE of 2a protons were selectively observed as shown in Fig. S7 (**1**), Fig. S8 (**3**) and Fig. S9 (**K2**). In contrast, a selective enhancement of NOE was not observed for **K4** as shown in Fig. S10, resulting in a difficulty to assign 2a and 2b protons.

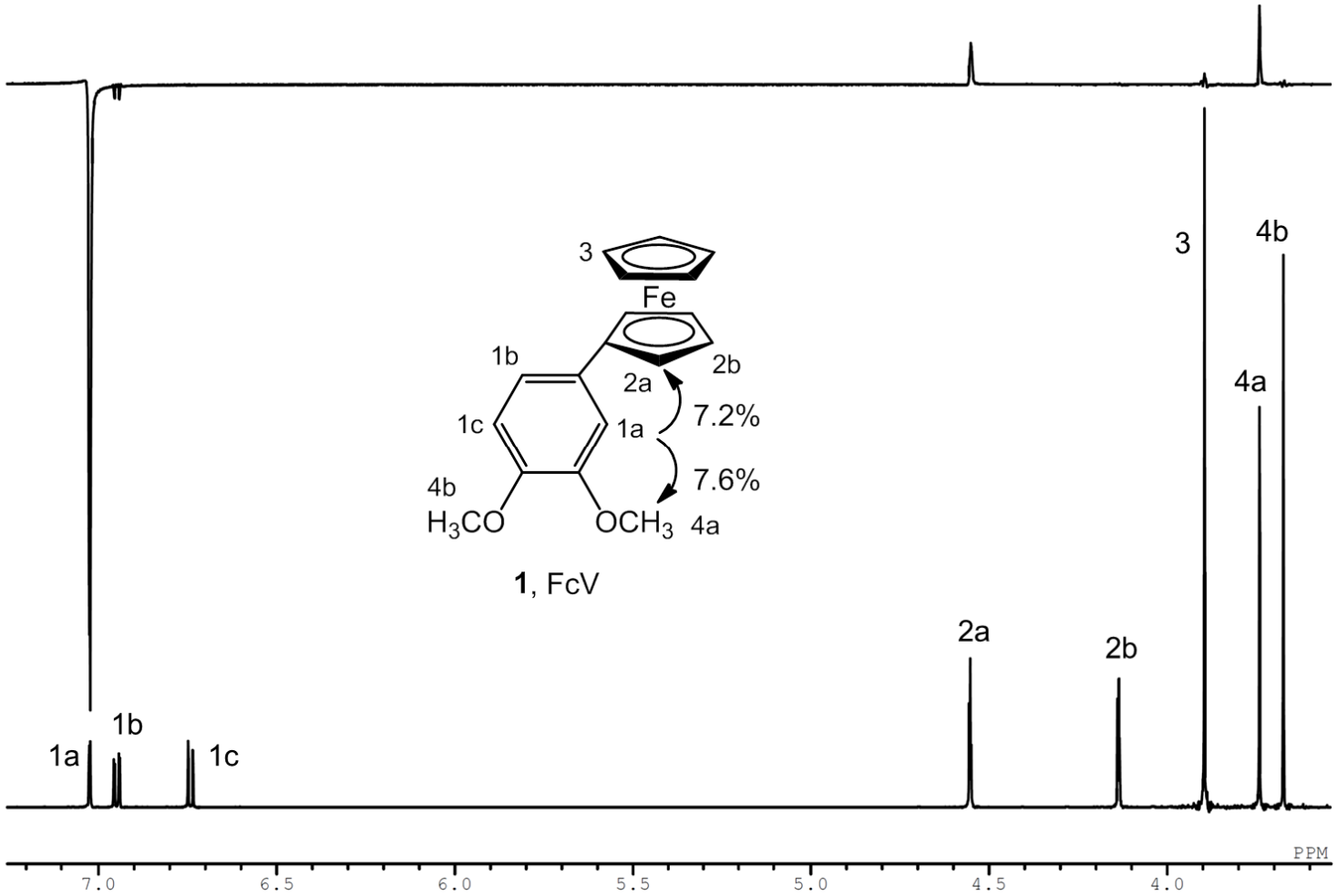

Fig. S7 Partial ^{1}H-NMR (bottom) and differential NOE (top) spectra of **1** in acetone-d_6. Nuclear Overhauser effects between protons are indicated as arrows.

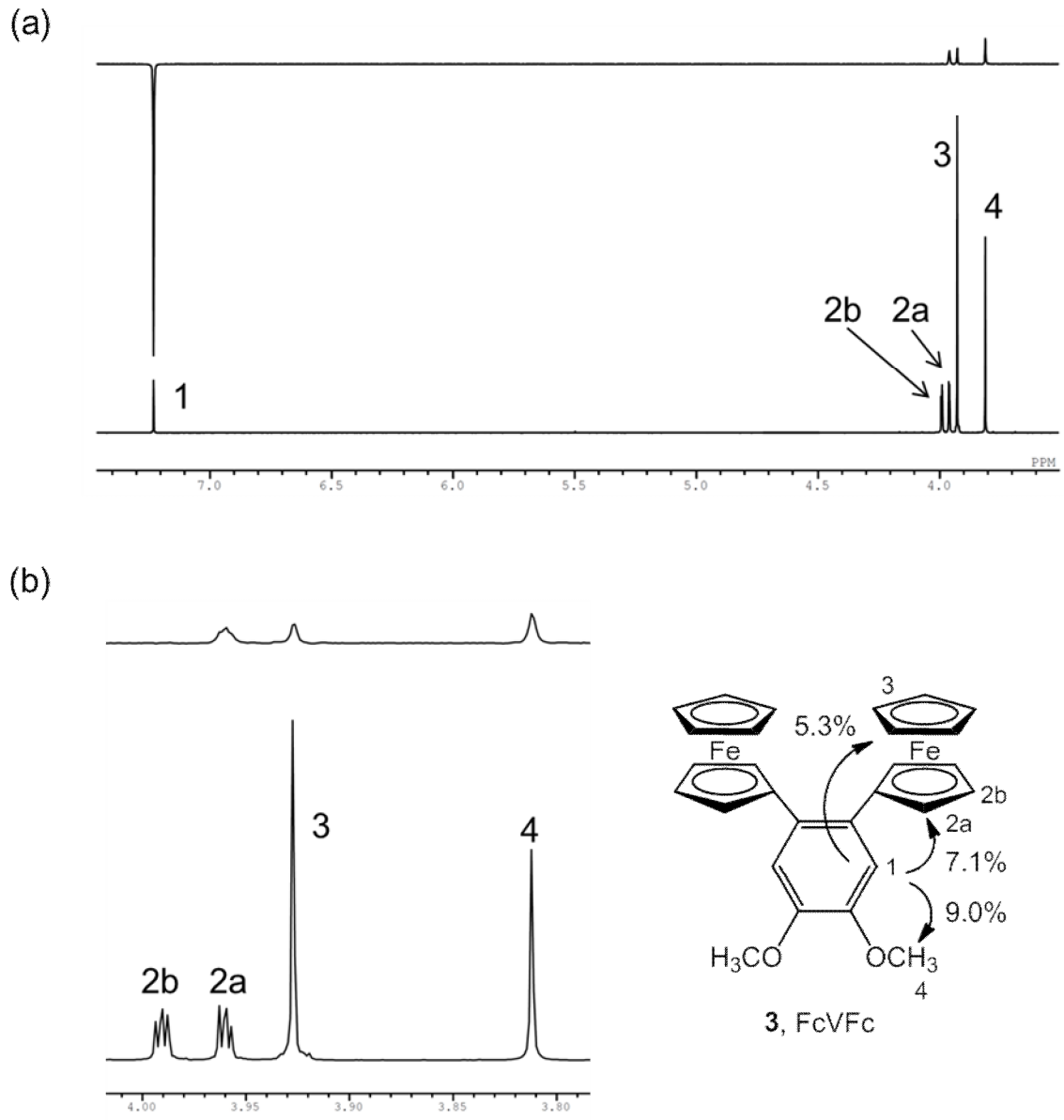

Fig. S8 (a) Partial ^{1}H-NMR (bottom) and differential NOE (top) spectra of **3** in acetone-d_6. (b) Enlarged view; nuclear Overhauser effects between protons are indicated as arrows.

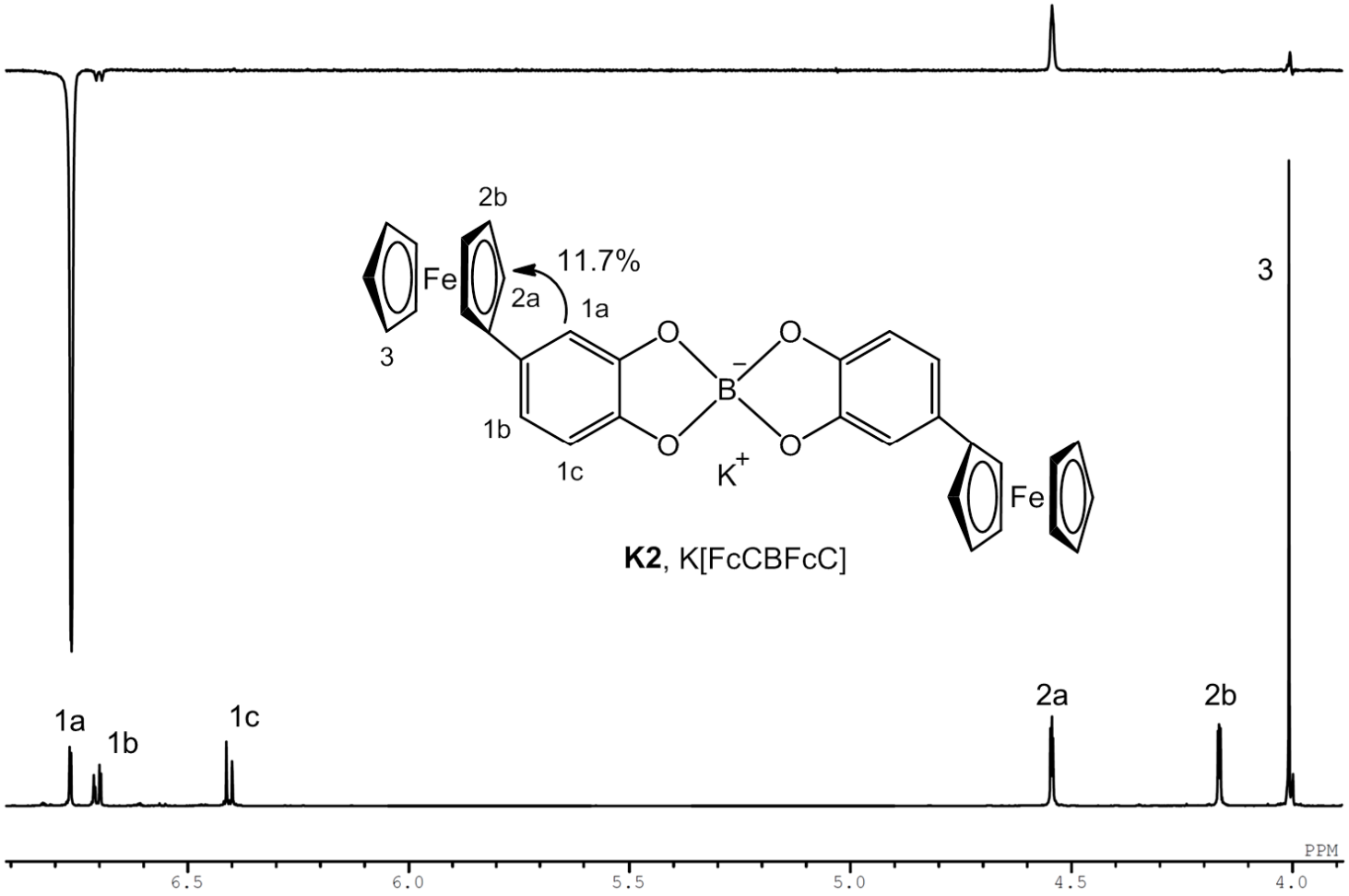

Fig. S9 Partial ^{1}H-NMR (bottom) and differential NOE (top) spectra of **K2** in acetone-d_6. Nuclear Overhauser effects between protons are indicated as arrows.

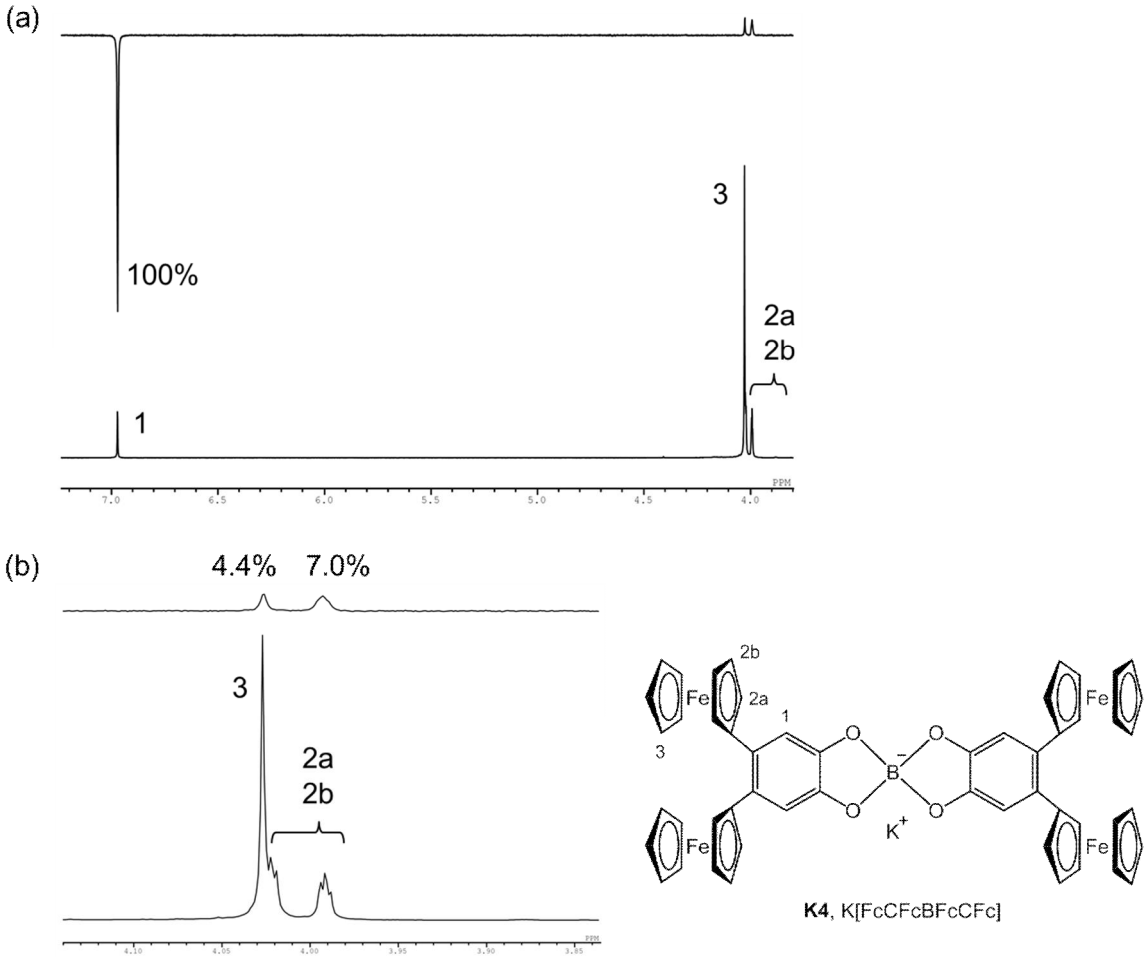

Fig. S10 (a) Partial ^{1}H-NMR (bottom) and differential NOE (top) spectra of **3** in acetone-d_6. (b) Enlarged view; percentage enhancements of nuclear Overhauser effects are indicated.

4. DFT Calculation Data

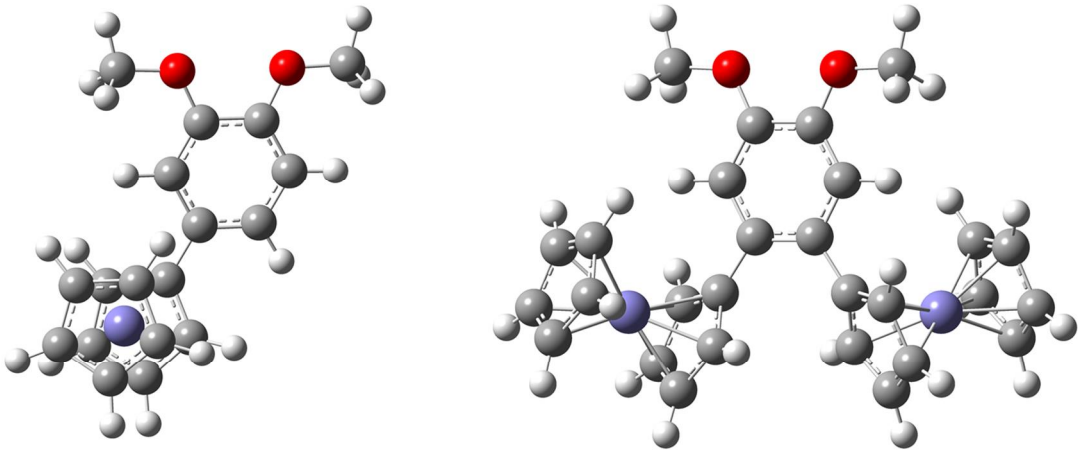

Fig. S11 Optimized gas-phase structures of **1** and **3** calculated using a DFT method (B3LYP/LanL2DZ (Fe atom) and 6-31G(d) (all other atoms) levels of theory).

Table S3. Coordinates of the optimized gas-phase geometries of **1** and **3** calculated using a DFT method (B3LYP/LanL2DZ (Fe atom) and 6-31G(d) (all other atoms) levels of theory).

Compound **1**

Atomic Number	Coordinates (Å)		
	X	Y	Z
26	-2.31619	-0.07346	0.036518
8	3.390472	1.87419	-0.47603
8	4.809153	-0.07421	0.483429
6	2.67198	2.970855	-1.00986
6	2.731823	0.689949	-0.3242
6	1.393396	0.477659	-0.63292
6	0.784535	-0.78204	-0.44381
6	-0.62983	-0.99802	-0.80479
6	-1.51821	-1.97189	-0.2366
6	-2.78403	-1.87255	-0.88677
6	-2.69787	-0.82991	-1.85726

6	-1.37921	-0.28869	-1.80386
6	-1.69712	1.188805	1.568496
6	-2.61207	0.216422	2.073634
6	-3.84798	0.366552	1.373493
6	-3.69722	1.432173	0.435226
6	-2.36755	1.939767	0.555401
6	5.625143	-1.10163	1.015903
6	3.509841	-0.37511	0.202455
6	2.911271	-1.61735	0.390574
6	1.563271	-1.82017	0.066198
1	1.830524	3.258341	-0.36413
1	2.291565	2.754715	-2.01764
1	3.383476	3.797235	-1.06241
1	0.789751	1.295932	-1.00676
1	-1.27847	-2.64062	0.579598
1	-3.66593	-2.45399	-0.65191
1	-3.49854	-0.48854	-2.50025
1	-1.00291	0.518904	-2.41778
1	-0.66231	1.30218	1.863841
1	-2.39551	-0.52585	2.830653
1	-4.73247	-0.24247	1.506333
1	-4.44753	1.773568	-0.26596
1	-1.9366	2.736296	-0.03711
1	5.719851	-1.94619	0.319483
1	5.237788	-1.47097	1.975388
1	6.607661	-0.65224	1.172643
1	3.489475	-2.44672	0.782077
1	1.133151	-2.80848	0.197327

Compound **3**

Atomic Number	Coordinates (Å)		
	X	Y	Z
26	-3.42868	-1.09547	-0.03039
26	3.428762	-1.09522	0.030698
8	1.179192	4.238728	0.549586
8	-1.17922	4.238721	-0.54998
6	2.451108	4.293361	1.169477
6	0.644208	3.011244	0.295728
6	1.263396	1.796847	0.55336
6	0.652756	0.555663	0.263544
6	1.424926	-0.67879	0.544005
6	1.522974	-1.85908	-0.26616
6	2.337832	-2.81367	0.411861
6	2.774211	-2.22806	1.638576
6	2.220238	-0.91595	1.71704
6	4.195776	0.467932	-1.11034
6	4.276007	-0.75708	-1.83798
6	5.086206	-1.66375	-1.08866
6	5.507626	-0.99897	0.102576
6	4.955974	0.318483	0.089809
6	-2.45163	4.293377	-1.16887
6	-0.64427	3.011238	-0.29605
6	-1.26343	1.79682	-0.55366
6	-0.65277	0.555652	-0.2638
6	-1.42494	-0.6788	-0.54423
6	-2.2206	-0.9159	-1.71703
6	-2.77449	-2.22804	-1.63851
6	-2.33771	-2.81375	-0.41197
6	-1.52268	-1.85917	0.265857
6	-4.19546	0.467759	1.110551
6	-4.95526	0.318564	-0.08989
6	-5.50735	-0.99873	-0.10287
6	-5.08648	-1.66371	1.088437
6	-4.27624	-0.75728	1.838059
1	3.230334	3.84355	0.538742

1	2.44693	3.790285	2.146112
1	2.670276	5.353625	1.309475
1	-2.36868	-0.21063	-2.52457
1	2.267929	1.781495	0.957864
1	-3.43178	-2.68526	-2.36651
1	-2.61258	-3.79181	-0.03921
1	1.06376	-1.99217	-1.23547
1	2.613024	-3.79161	0.039023
1	3.431393	-2.68516	2.366758
1	2.367862	-0.21067	2.524653
1	3.618935	1.337203	-1.39665
1	3.779832	-0.97273	-2.77503
1	5.310128	-2.68759	-1.35816
1	6.109525	-1.42922	0.892266
1	5.077806	1.06361	0.865505
1	-3.23029	3.843208	-0.5377
1	-2.44813	3.79066	-2.1457
1	-2.67107	5.353655	-1.30833
1	-1.06318	-1.99235	1.235022
1	-2.26797	1.781434	-0.95815
1	-3.61832	1.336791	1.397045
1	-5.07688	1.063837	-0.86548
1	-6.10905	-1.42871	-0.89286
1	-5.31067	-2.68747	1.358006
1	-3.78056	-0.97311	2.775329

Table S4. DFT-calculated molecular orbital compositions of **1** and **3** in gas phase.

Compound **1**

MO	*E* /eV	Composition / %		
		Fe	Cp	Veratrole
85	0.59248537	81	8	11
84	0.441295582	67	13	20
83	0.40445303	45	20	36
82	0.37997014	23	4	74
81	0.011003492	58	41	1
80 (LUMO)	-0.318017101	38	26	36
79 (HOMO)	-5.073078268	41	11	48
78	-5.286083255	86	14	0
77	-5.419677401	47	15	37
76	-6.136953919	7	19	74
75	-6.33147216	88	9	3

Compound **3**

MO	*E* /eV	Composition / %		
		Fe	Cp	Veratrole
129	0.446484	45	15	40
128	0.433018	88	5	7
127	0.418447	73	11	16
126	0.369519	31	35	34
125	0.058908	57	40	3
124	-0.0501	60	40	1
123	-0.20583	40	27	33
122 (LUMO)	-0.40455	39	28	33
121 (HOMO)	-5.02055	40	15	45
120	-5.24535	82	13	5
119	-5.27339	86	14	0
118	-5.29326	86	14	0
117	-5.42554	52	18	31
116	-6.02453	12	31	57
115	-6.32041	90	8	3
114	-6.34019	87	10	3

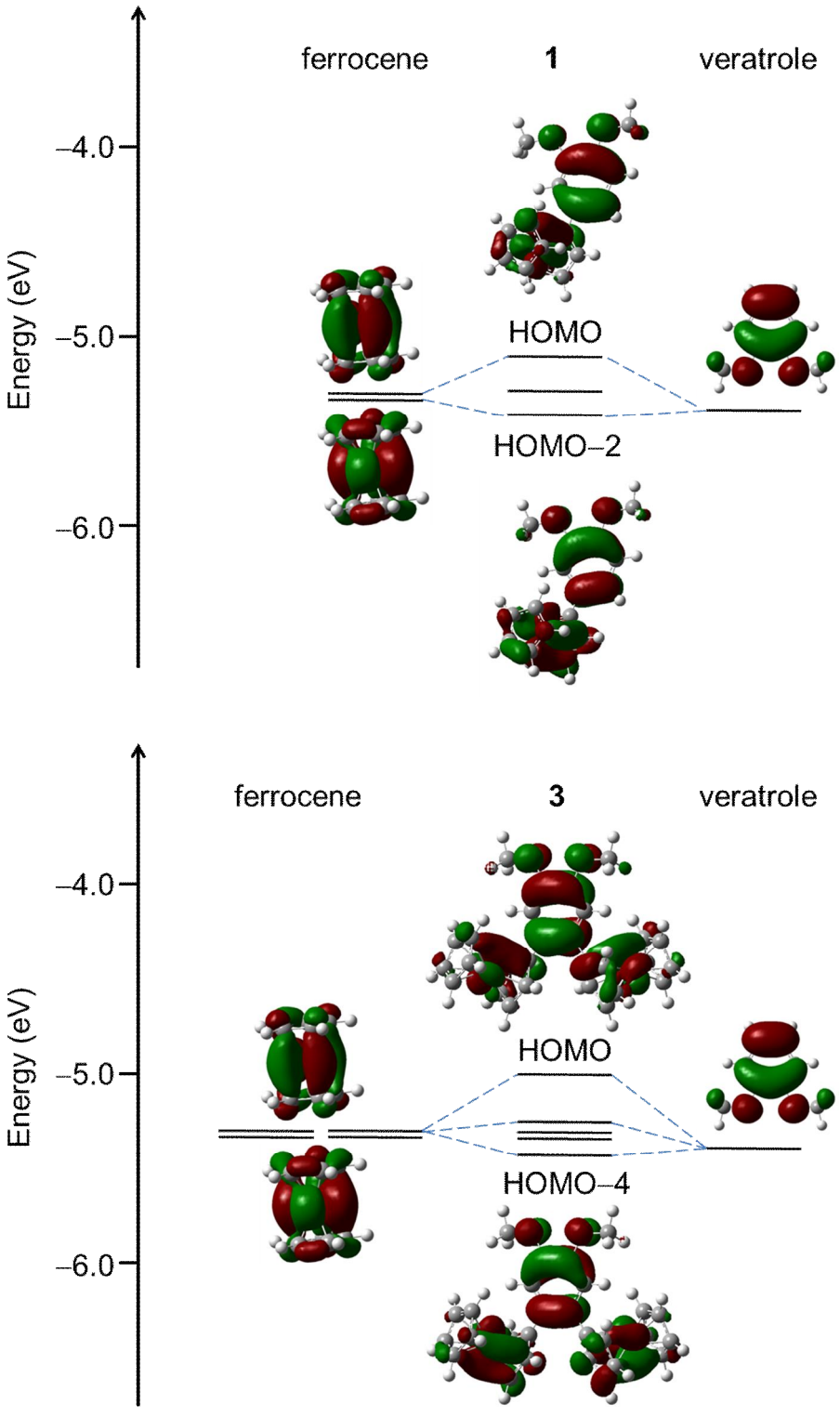

Fig. S12 Selected molecular orbital contributions and energy diagrams for **1**, **3**, ferrocene, and veratrole in gas phase, calculated using a DFT method (B3LYP/LanL2DZ (Fe atom) and 6-31G(d) (all other atoms) levels of theory) (isosurface values 0.02 au).

Table S5. TD-DFT-predicted vertical excitation energies for **1** and **3** in gas phase.

Compound **1**

#	*f*	eV	nm	Transition	Coefficients
3	0.0010	2.5698	482.48	75 -> 80	0.38626
				75 -> 83	0.16942
				75 -> 84	-0.14253
				77 -> 80	-0.15537
				77 -> 81	0.11355
				78 -> 80	-0.13877
				78 -> 81	-0.36442
				79 -> 80	-0.20741
				79 -> 81	0.12504
7	0.1861	4.3740	283.46	77 -> 80	0.50559
				79 -> 80	-0.41653
				79 -> 83	-0.16703
10	0.1045	4.5742	271.05	77 -> 80	-0.12989
				77 -> 83	0.19266
				77 -> 84	-0.12561
				78 -> 80	-0.10527
				78 -> 83	0.1728
				79 -> 80	-0.27422
				79 -> 82	0.22995
				79 -> 83	0.33715
				79 -> 84	-0.28351
				79 -> 85	-0.10313
11	0.0584	4.7616	260.38	76 -> 80	-0.31091
				77 -> 83	-0.12069
				77 -> 84	0.12681
				79 -> 80	0.12315
				79 -> 82	0.51025
				79 -> 83	-0.1986

Compound **3**

#	*f*	eV	nm	Transition	Coefficients
5	0.0017	2.5649	483.38	114 ->123	-0.26831
				114 ->129	0.12891
				115 ->122	0.2838
				115 ->126	0.17364
				117 ->124	0.10497
				118 ->125	-0.25694
				119 ->122	0.14121
				119 ->124	-0.25371
				120 ->123	0.18299
				121 ->122	0.13825
				121 ->124	0.10621
13	0.0115	4.1743	297.02	117 ->123	-0.11720
				120 ->122	-0.36155
				120 ->126	0.11109
				121 ->123	0.56379
14	0.3278	4.2308	293.05	117 ->122	-0.23949
				120 ->123	-0.20658
				121 ->122	0.59334
16	0.0021	4.3860	282.68	118 ->123	0.33235
				119 ->122	0.49314
				119 ->126	-0.28215
18	0.0028	4.4204	280.48	117 ->122	0.49156
				117 ->124	0.1775
				120 ->123	-0.26838
				121 ->124	-0.14957
				121 ->126	-0.27265
20	0.0732	4.5471	272.67	116 ->122	-0.13828
				117 ->123	-0.35273
				120 ->122	0.36066
				120 ->126	-0.25543
				121 ->123	0.17589
				121 ->125	0.10103
				121 ->127	-0.14454

				121 ->129	0.19805
21	0.0729	4.63	267.78	117 ->126	-0.11939
				120 ->123	0.42953
				120 ->125	0.12189
				120 ->127	-0.17145
				120 ->129	0.23286
				121 ->126	-0.39704
22	0.0011	4.6537	266.42	116 ->122	-0.16247
				117 ->123	0.43072
				117 ->125	0.13201
				120 ->126	-0.18639
				121 ->127	-0.25456
				121 ->129	0.3408
26	0.0028	4.8297	256.71	116 ->124	0.14493
				117 ->124	-0.12913
				117 ->125	0.39615
				118 ->124	0.14172
				120 ->124	0.38
				120 ->125	-0.14052
				121 ->125	0.1494
				121 ->129	-0.10041
29	0.0050	4.8579	255.22	118 ->125	0.46984
				119 ->124	-0.46391
				120 ->125	-0.11

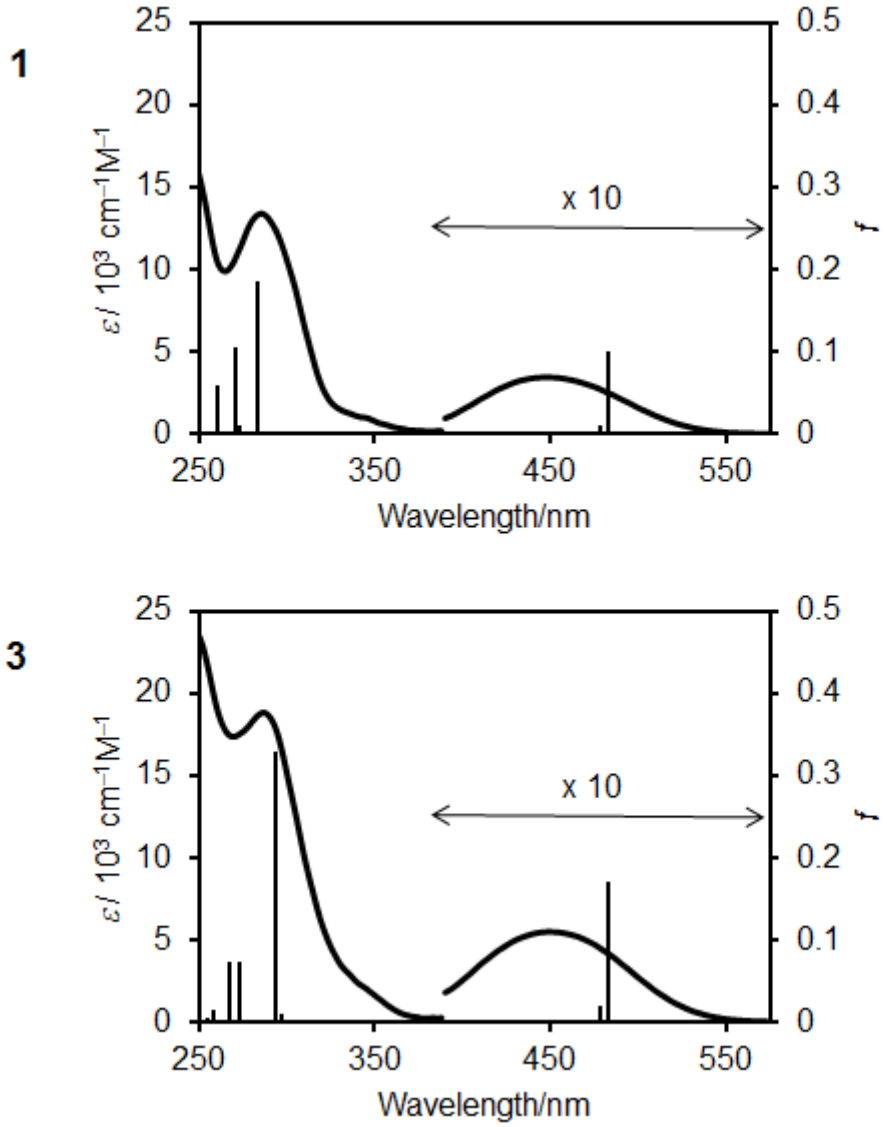

Fig. S13 Experimental UV-vis spectra of **1** and **3** in CH_2Cl_2 (black lines), and TD-DFT-calculated transition energies and oscillation strengths (*f*) (bars).

5. Vis-NIR Spectra of 1, K2, 3 and K4

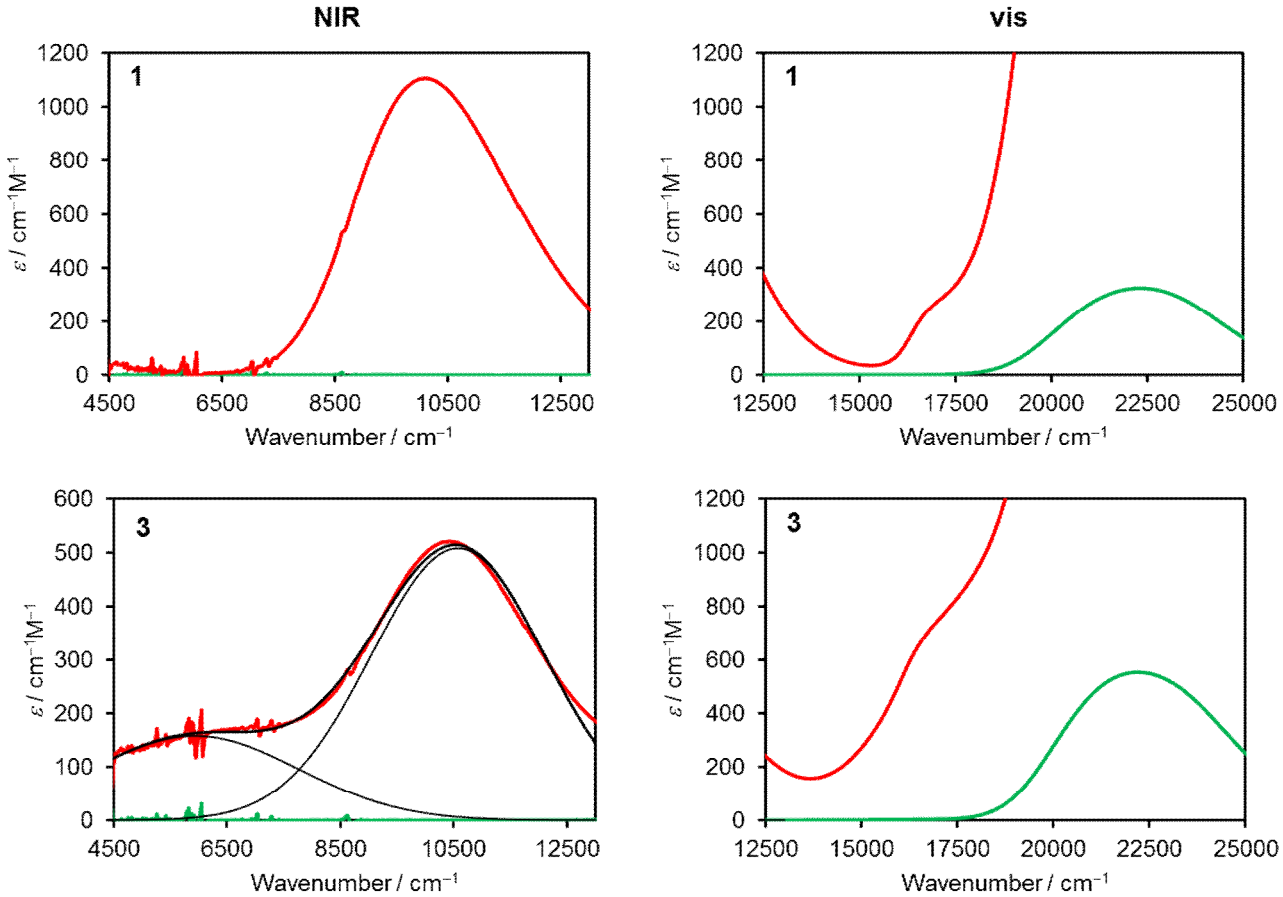

Fig. S14 Vis (left) and NIR (right) spectra of **1** and **3** in the absence (green line) and presence (red line) of 1 equiv of $Ag(SbF_6)$ in CH_2Cl_2, with Gaussian deconvolution (black line) and the sum (black bold line). The region below 4500 cm^{-1} is not shown because of overlap of the solvent absorption.

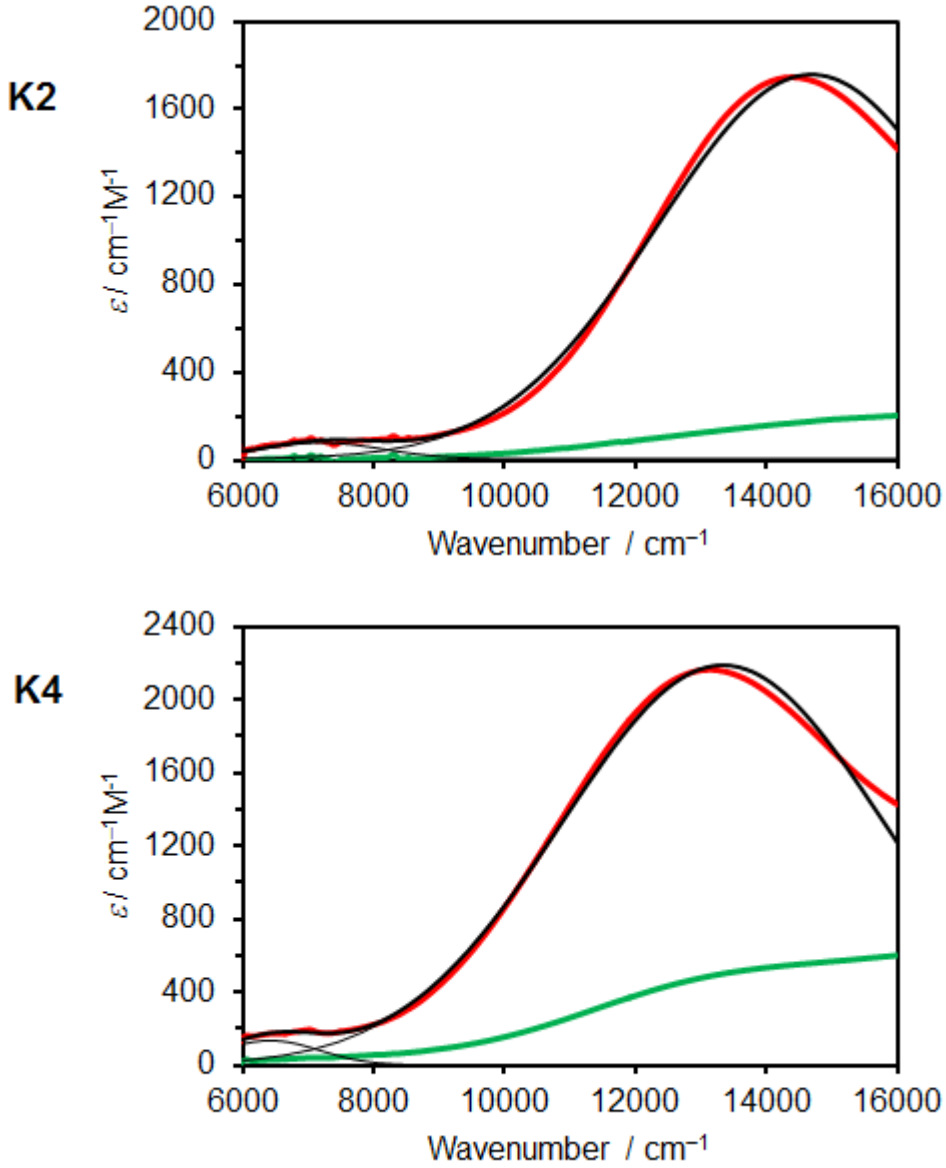

Fig. S15 NIR spectra of **K2** and **K4** in the absence (green line) and presence (red line) of 1 equiv of $Ag(SbF_6)$ in DMF, with Gaussian deconvolution (black line) and the sum (black bold line). The region below 6000 cm^{-1} is not shown because of overlap of the solvent absorption.

6. Electrochemical Data

Table S6. Electrochemical date for **1** and **3** in CH_2Cl_2.[a]

Compound	Counter Anion of Electrolyte	$E_{1/2}^1$	$E_{1/2}^2$	$\Delta E_{1/2}$[b]
1	PF_6^-	8	-	-
1	$B(C_6F_5)_4^-$	–47	-	-
3	PF_6^-	–74	93	167
3	$B(C_6F_5)_4^-$	–124	139	263

[a] Potentials in mV vs. Fc^+/Fc. Use of tetrabutylammonium salts as electrolytes. [b] $\Delta E_{1/2}$ = potential difference between two redox processes.

Table S7. Electrochemical date for **1**, **2K** and **3** in DMF.[a]

# of Fc	Compound	Counter Anion of Electrolyte	$E_{1/2}^1$	$E_{1/2}^2$	$E_{1/2}^3$	$E_{1/2}^4$
mono	**1**	PF_6^-	–30	-	-	-
mono	**1**	$B(C_6F_5)_4$	–32	-	-	-
di	**K2**	PF_6^-	–108	194	-	-
di	**K2**	$B(C_6F_5)_4$	–120	192	-	-
di	**3**	PF_6^-	–48	68	-	-
di	**3**	$B(C_6F_5)_4^-$	–48	78	-	-
tetra	**K4**	PF_6^-	–121	22	103	196
tetra	**K4**	$B(C_6F_5)_4^-$	–127	22	97	205

[a] Potentials in mV vs. Fc^+/Fc. Use of tetrabutylammonium salts as electrolytes. [b] $\Delta E_{1/2}$ = potential difference between two redox processes.